# Propagation of an electromagnetic pulse through a waveguide with a barrier: A time domain solution within classical electrodynamics

Thorsten Emig

*Institut für Theoretische Physik, Universität zu Köln, D-50923 Köln, Germany*

(November 1, 1996)

An electromagnetic truncated Gaussian pulse propagates through a waveguide with piecewise different dielectric constants. The waveguide contains a barrier, namely a region of a lower dielectric constant compared to the neighboring regions. This set-up yields a purely imaginary wave vector in the region of the barrier ('electromagnetic tunneling'). We exactly calculate the time-dependent Green's function for a slightly simplified dispersion relation. In order to observe the plain tunneling effect we neglect the distortions caused by the wave guide in obtaining the transmitted pulse. The wave front of the pulse travels with the vacuum speed of light. Nevertheless, behind the barrier, the maximum of the transmitted pulse turns up at an earlier time than in the case without an barrier. This effect will be explained in terms of the energy flow across the barrier. The solutions obtained reproduce the shape of the pulses measured in the tunneling experiments of Enders and Nimtz [4–8].

PACS numbers: 03.50.De, 73.40.Gk, 03.40.Kf

## I. INTRODUCTION

Tunneling is, like interference, a characteristic property of waves. This effect occurs both in non-relativistic quantum mechanics and in electrodynamics. Although the time dependent differential equations of both theories are fundamentally different in their structure, theoretical calculations yield analogous results for the traversal time of the maximum of a wave packet's modulus. These calculations are based on the stationary phase approximation [1,2] as well as on a scattering ansatz [3]. For sufficiently long barriers, the time delay is independent of the thickness and, thus, can correspond to arbitrary large effective velocities of the maximum of a pulse for crossing the barrier. This prediction is in agreement with results obtained by Nimtz and Enders in tunneling experiments with evanescent microwaves in a waveguide with a frequency below cut-off [4–8]. In these experiments the evanescent waveguide region, i.e. the barrier, is realized by an undersized region in between normal sized regions of a waveguide line. Due to the inhomogeneous cross section of the waveguide, we couldn't obtain an analytic expression for the transmission coefficient. Therefore, a recent microwave experiment [9] studied a barrier produced by a low-dielectric-constant ($\epsilon_2$) region which was placed in a rectangular waveguide of the same cross section, filled with a higher dielectric constant $\epsilon_1$. This experimental set-up is illustrated in Fig. 1. The relation between wave number $k$ and frequency $\omega$ is given by the dispersion formula (with the vacuum speed of light set to $c = 1$)

$$k = \sqrt{\epsilon}\sqrt{\omega^2 - \omega_c^2/\epsilon} \tag{1.1}$$

where $\omega_c$ represents the cut-off frequency of the empty waveguide and $\epsilon$ is the variable dielectric constant [10]. Therefore a wave of frequency $\omega_0$ with $\omega_c^2/\epsilon_1 < \omega_0^2 <$

$\omega_c^2/\epsilon_2$ possesses a real wave number $k$ outside the barrier, but on entering the tunnel region with a lower dielectric constant $k$ becomes imaginary, and the wave will spatially decay.

In this paper we will consider the electrodynamic tunneling for a barrier given by a variable dielectric constant. This set-up is amenable to a rigorous mathematical description. It was theoretically investigated first by Martin and Landauer [3]. They concentrated on the tunneling of a Gaussian pulse with a narrow frequency range. Using a scattering ansatz they showed that the time delay of the center of mass depends only on the frequency derivative of the phase of the transmission coefficient. For sufficiently long barriers, this delay becomes independent of thickness and thus corresponds to an arbitrary large effective velocity of the center of mass for crossing the tunnel region, which is known as the Hartman effect [1] and has been experimentally verified first by Enders and Nimtz [5].
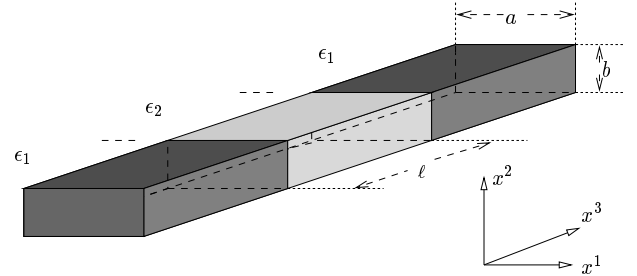


FIG. 1. The set-up of the considered waveguide.

We want to examine how this effect is related to causality. To carry out this goal, the fundamental solution of the given set-up, the retarded Green's function, will be constructed analytically assuming causality. This means

1

that this function vanishes outside the past light cone, i.e. the wave front travels with the vacuum speed of light. With the aid of this solution we will give an analytic expression for the entire transmitted pulse, which has the observed superluminal property of the center of mass. In addition this allows us to determine the deformation of the pulse caused by crossing the barrier. It is assumed that the initial pulse is given by a truncated Gaussian wave packet located only to the left of the barrier.

## II. GREEN'S FUNCTION

### A. The Model

The Green's function will be obtained using a Laplace transform. The structure of the dipersion formula (1.1) prevents an analytic inversion of this transformation because of the different coefficients in front of $\omega^2$ outside and inside the barrier, respectively. Therefore we consider in this paper a simplified model for the electromagnetic tunneling effect with dispersion formulas given by

$$k = \sqrt{\omega^2 - m_1^2}, \quad \kappa = \sqrt{\omega^2 - m_2^2} \qquad (2.1)$$

with $\sqrt{\epsilon}$ coefficients dropped and cut-off frequencies $m_1 = \omega_c/\sqrt{\epsilon_1}$ and $m_2 = \omega_c/\sqrt{\epsilon_2}$ outside and inside the barrier, respectively. The transmission coefficient of the barrier does not change qualitatively under this simplification. The model given by these dispersion formulas, together with the Maxwell equations, still represents an electrodynamic case of tunneling. Within this model the velocity of a wave front $\lim_{k\to\infty} \omega(k)/k = 1$ is always given by the vacuum speed of light and it is assumed that the dielectric medium influences only the cut-off frequencies themselves. A similar model consisting of a classical scalar field which satisfies the one-dimensional relativistic Klein-Gordon equation with a rectangular potential barrier was investigated by Deutch and Low [11]. Under the condition that the tunneling amplitude is very small, they found an approximate solution given by a Gaussian wave packet, which turns up on the right hand side of the barrier as if its maximum took zero time to cross the barrier. Our goal here is to find an exact solution of the Maxwell equations yielding exact values for the tunneling time of the maximum of a Gaussian wave packet, which can be compared to the approximate results given by Martin and Landauer. Furthermore, taking truncated wave packets of variable variance, the influence of these attributes on the tunneling time will be studied.

Suppose that an electromagnetic pulse has been generated in the region to the left of the barrier by an appropriate current which has vanished already before the wave front of the pulse reaches the left end of the barrier. The propagation of this pulse is then determined by the dispersion formulas together with the Maxwell equations with vanishing charge current. One can obtain the propagated field behind the barrier by solving these equations with the pulse located in front of the barrier as initial condition. This can be done with the aid of the retarded Green's function. In the case of the electromagnetic field, this fundamental solution can be written as an antisymmetric tensor $G_{\bar{x}\alpha\beta}$, $(\alpha, \beta = 0, \ldots, 3)$, satisfying the four dimensional wave equation with the Dirac distribution at the fixed space-time position $\bar{x}$ as inhomogeneity

$$\Box G_{\bar{x}} = -\delta_{\bar{x}}, \qquad (2.2)$$

where $\Box = \partial_0^2 - \partial_1^2 - \partial_2^2 - \partial_3^2$ is the Laplace-Beltrami-operator of the Minkowskian space time [12]. Beyond that, $G_{\bar{x}}$ must allow for the following boundary conditions: First, it has to vanish outside the past light cone at $\bar{x}$, second its six components have to jump in the respective correct manner at the two boundaries between the propagating and the evanescent region and must take into account the metallic boundary conditions on the surface of the waveguide. In the next section, we will give a solution of this boundary value problem where the axial magnetic component $G_{\bar{x}12}$ of Green's function shall serve as example. Given the relevant field components in front of the barrier at the time $x^0 = 0$, the expression

$$B_3(\bar{x}) = \int_N \left[ G_{\bar{x}12,1}E_2 - G_{\bar{x}12,2}E_1 - G_{\bar{x}12,0}B_3 \right] dx^1 dx^2 dx^3$$

$$(2.3)$$

yields the time evolution of the $B_3$ component of the magnetic field behind the barrier $\bar{x}^3 > \ell/2$ in terms of partial derivatives $G_{\bar{x}\alpha\beta,\gamma}$ of Green's function. The three-dimensional domain $N = \{x \in \mathbf{R}^4 | 0 \leq x^1 \leq a, 0 \leq x^2 \leq b, x^0 = 0\}$ of integration is the interior of the whole waveguide line at time $x^0 = 0$.

### B. Analysis

We solve the time dependent wave equation (2.2) by a Laplace transform relative to the time $x^0$ for a fixed $\bar{x}$ with the property $\bar{x}^0 > 0$. The Laplace transform yields, after inversion, a function in the time domain which vanishes *until* a certain time is reached. Therefore this method is only suitable to get the advanced Green's function. The retarded Green's function, though, can then be obtained by a simple time reflection.

The transformed components of Green's function are defined by

$$\tilde{G}_{\bar{x}\alpha\beta}(\omega) = \mathcal{L}[G_{\bar{x}\alpha\beta}] = \int_0^\infty e^{i\omega x^0} G_{\bar{x}\alpha\beta} dx^0 \qquad (2.4)$$

where $\mathcal{L}$ denotes the Laplace transform with $\omega$ in the upper half plane of complex numbers.

For a waveguide with perfectly conducting walls given by the surface $S$, the boundary condition for the electromagnetic field reads [10]

$$(\vec{n} \times \vec{E})_{|S} = 0, \quad (\vec{n} \cdot \vec{B})_{|S} = 0 \qquad (2.5)$$

where $\vec{n}$ is the vector normal to the surface $S$. This condition is satisfied if one uses a Green's function which is invariant relative to the reflections at the four walls of the rectangular waveguide. This invariant Green's function can be decomposed into the characteristic modes of the waveguide. The result for the Laplace transformed components can be written as

$$\tilde{G}_{\bar{x}\alpha\beta} = \frac{1}{2\pi ab} \sum_{\iota,\eta=-\infty}^{\infty} f_{\alpha\beta} e^{-i(x^1\pi/a\iota + x^2\pi/b\eta)} e^{i\omega\bar{x}^0} \tilde{g}_{\alpha\beta}(\bar{x}^3, x^3)$$

$$(2.6)$$

introducing the antisymmetric tensor

$$f_{\alpha\beta} = \begin{pmatrix} 0 & ic_1 s_2 & is_1 c_2 & -s_1 s_2 \\ -ic_1 s_2 & 0 & c_1 c_2 & ic_1 s_2 \\ -is_1 c_2 & -c_1 c_2 & 0 & is_1 c_2 \\ s_1 s_2 & -ic_1 s_2 & -is_1 c_2 & 0 \end{pmatrix} \qquad (2.7)$$

with

$$c_1 := \cos(\bar{x}^1 \iota\pi/a), \quad s_1 := \sin(\bar{x}^1 \iota\pi/a), \qquad (2.8)$$
$$c_2 := \cos(\bar{x}^2 \eta\pi/b), \quad s_2 := \sin(\bar{x}^2 \eta\pi/b). \qquad (2.9)$$

This tensor describes the $x^1$- and $x^2$-dependence of the modes represented by its respective pairs of numbers $(\iota, \eta)$. Here we have introduced a one dimensional Green's function $\tilde{g}_{\alpha\beta}(\bar{x}^3, x^3)$ to account for the dependence on the axial coordinate $x^3$. Only this function contains the dependence on the frequency and will therefore define the time evolution of the field. Applying the transformed wave equation (2.2) to Eq. (2.6), we find that the one dimensional Green's function has to be a solution of the ordinary differential equation given by

$$\left[ \frac{d^2}{d(x^3)^2} + \omega^2 - m^2(x^3) \right] \tilde{g}_{\alpha\beta}(\bar{x}^3, x^3) = \delta(x^3 - \bar{x}^3)$$

$$(2.10)$$

with the jumping cut-off frequency determined by the simplified dispersion formulas (2.1), i.e.

$$m(x^3) = \begin{cases} m_1 = \omega_c/\sqrt{\epsilon_1}, & |x^3| \geq \ell/2 \\ m_2 = \omega_c/\sqrt{\epsilon_2}, & |x^3| < \ell/2, \end{cases} \qquad (2.11)$$

with $\omega_c = \pi\sqrt{\iota^2/a^2 + \eta^2/b^2}$ for a rectangular waveguide. Notice that the cut-off frequencies $m_1$ and $m_2$ change with the type of mode. Thus the one dimensional Green's function also depends on the numbers $(\iota, \eta)$. In Eq. (2.10) no boundary terms at zero time emerge from the Laplace transform of the second time derivative due to the vanishing of the advanced Green's function for $x^0 < \bar{x}^0$ and the property $\bar{x}^0 > 0$.

The one dimensional Green's function for (2.10) can be constructed from two linear independent solutions of

the corresponding homogeneous equation. These can be chosen as a plane wave traveling from the left-hand side and the right-hand side, respectively, toward the barrier, i.e.

$$\phi_{\alpha\beta}^{(1)}(x^3) = \begin{cases} \epsilon_{\alpha\beta} e^{ikx^3} + R_{\alpha\beta} e^{-ikx^3}, & x^3 \leq -\ell/2, \\ A_{\alpha\beta} e^{i\kappa x^3} + B_{\alpha\beta} e^{-i\kappa x^3}, & |x^3| < \ell/2, \\ T_{\alpha\beta} e^{ikx^3}, & x^3 \geq \ell/2, \end{cases} \qquad (2.12)$$

and

$$\phi_{\alpha\beta}^{(2)}(x^3) = \begin{cases} T_{\alpha\beta} e^{-ikx^3}, & x^3 \leq -\ell/2, \\ A_{\alpha\beta} e^{-i\kappa x^3} + B_{\alpha\beta} e^{i\kappa x^3}, & |x^3| < \ell/2, \\ \epsilon_{\alpha\beta} e^{-ikx^3} + R_{\alpha\beta} e^{ikx^3}, & x^3 \geq \ell/2. \end{cases} \qquad (2.13)$$

with the total antisymmetric tensor $\epsilon_{\alpha\beta}$. The wave numbers $k$ and $\kappa$ are given by the dispersion formulas (2.1). Due to the upper half plane analyticity of a Laplace transformed function, the square roots in these equations have to be chosen analytic in the upper $\omega$ half plane. Hence the wave numbers always have a positive imaginary part. The respective coefficients $R_{\alpha\beta}$, $A_{\alpha\beta}$, $B_{\alpha\beta}$ and $T_{\alpha\beta}$ are uniquely determined by the boundary conditions at the two planes defining the evanescent region between $x^3 = -\ell/2$ and $x^3 = \ell/2$. The coefficients of both solutions are assumed to be equal because of the symmetry of the barrier relative to $x^3 = 0$. Taking into account that the imaginary part of $k$ is positive, the asymptotic behavior of the two solutions looks like

$$\lim_{x^3 \to -\infty} \phi_{\alpha\beta}^{(2)}(x^3) = 0, \quad \lim_{x^3 \to \infty} \phi_{\alpha\beta}^{(1)}(x^3) = 0. \qquad (2.14)$$

Therefore we can construct Green's function in the upper $\omega$ half plane as

$$\tilde{g}_{\alpha\beta}(\bar{x}^3, x^3) = \frac{1}{W_{\alpha\beta}} \cdot \begin{cases} \phi_{\alpha\beta}^{(1)}(\bar{x}^3)\phi_{\alpha\beta}^{(2)}(x^3), & \bar{x}^3 \geq x^3 \\ \phi_{\alpha\beta}^{(2)}(\bar{x}^3)\phi_{\alpha\beta}^{(1)}(x^3), & \bar{x}^3 \leq x^3 \end{cases} \qquad (2.15)$$

with the Wronskian $W_{\alpha\beta}$ of $\phi_{\alpha\beta}^{(1)}$ and $\phi_{\alpha\beta}^{(2)}$ defined by

$$W_{\alpha\beta} = \phi_{\alpha\beta}^{(2)} \frac{d\phi_{\alpha\beta}^{(1)}}{dx^3} - \phi_{\alpha\beta}^{(1)} \frac{d\phi_{\alpha\beta}^{(2)}}{dx^3}. \qquad (2.16)$$

The case $x^3 < \bar{x}^3$ with $x^3 < -\ell/2$ and $\bar{x}^3 > \ell/2$ is the interesting one for the investigation of the tunneling time problem for wave packets. In this case Green's function is suitable to calculate the field behind the barrier for a pulse assumed to be located initially only in the front of the barrier. In this case the Green's function reads

$$\tilde{g}_{\alpha\beta}(\bar{x}^3, x^3) = \frac{1}{2ik} T_{\alpha\beta} e^{ik(\bar{x}^3 - x^3)}. \qquad (2.17)$$

We now must consider the respective matching conditions for the components of the electromagnetic field to evaluate the coefficients of the two solutions. For simplicity let us only look at the calculations for the component $B_3$. This component has to be continuous at $x^3 = -\ell/2$ and $x^3 = \ell/2$. Furthermore we need the behavior of its

partial derivative perpendicular to the boundary-planes of the barrier. The transverse components $B_1$ and $B_2$ are continuous at any position of the two boundary-planes. Hence its partial derivatives parallel to the boundary-planes, i.e. the $x^1$- and $x^2$-derivatives, also have to be continuous at these planes. The equation $\mathrm{div}\vec{B} = 0$ shows that the $x^3$-derivative of the component $B_3$ is continuous at the boundary-planes, too. These four continuity conditions together yield the coefficients of the corresponding functions $\phi_{12}^{(1)}$ and $\phi_{12}^{(2)}$:

$$R_{12} = D^{-1}e^{-ik\ell}\left(1 - e^{2i\kappa\ell}\right)\left(k^2 - \kappa^2\right) \qquad (2.18)$$

$$A_{12} = D^{-1}2k(k+\kappa)e^{i(\kappa-k)\ell/2} \qquad (2.19)$$

$$B_{12} = -D^{-1}2k(k-\kappa)e^{i(3\kappa-k)\ell/2} \qquad (2.20)$$

$$T_{12} = D^{-1}4k\kappa e^{i(\kappa-k)\ell} \qquad (2.21)$$

with the common denominator

$$D = (k+\kappa)^2 - (k-\kappa)^2e^{2i\kappa\ell}. \qquad (2.22)$$

Due to the absence of upper half plane zeros of $D$ the coefficients are analytic in this half plane.

We find the one dimensional retarded Green's function in the time domain after a time reflection. The inverse Laplace transform yields, for $t := \bar{x}^0 - x^0 \geq 0$,

$$g_{\alpha\beta}(t, \bar{x}^3, x^3) = \frac{1}{2\pi}\int_{-\infty+is}^{\infty+is} e^{-i\omega t}\tilde{g}_{\alpha\beta}(\bar{x}^3, x^3)d\omega \quad (2.23)$$

with $\tilde{g}_{\alpha\beta}(\bar{x}^3, x^3)$ given by Eq. (2.17).

In the case of the component $B_3$ we now have to consider the transmission coefficient $T_{12}$ given in (2.21). Note that the expression $k + \kappa$ never vanishes in the upper $\omega$ half plane. Thus, expanding the right-hand side of (2.21) with $1/(k+\kappa)^2$, we find

$$T_{12} = \frac{4k\kappa}{(k+\kappa)^2}e^{i(\kappa-k)\ell}\frac{1}{1 - \left(\frac{k-\kappa}{k+\kappa}\right)^2 e^{2i\kappa\ell}}. \qquad (2.24)$$

The term $(k-\kappa)/(k+\kappa)$ is bounded in the upper $\omega$ half plane by 1 and the imaginary part of $\kappa$ is always positive in this half plane. Thus the transmission coefficient can be written as a geometric series

$$T_{12} = 4k\kappa e^{-ik\ell}\sum_{\nu=0}^{\infty}\frac{(k-\kappa)^{2\nu}}{(k+\kappa)^{2\nu+2}}e^{i\kappa\ell(2\nu+1)}. \qquad (2.25)$$

At this stage we need the simplified dispersion formulas (2.1) for an analytic inversion of the Laplace transform. Expanding each term of the series with $(k+\kappa)^{2\nu}$ cancels the $\omega^2$ terms in the numerator. Thus the transformed Green's function (2.17) becomes

$$\tilde{g}_{12}(\bar{x}^3, x^3) = -2i\kappa^2 e^{ik(\bar{x}^3-x^3-\ell)}$$
$$\times \sum_{\nu=0}^{\infty}\frac{1}{\kappa}\frac{(m_2^2 - m_1^2)^{2\nu}}{(k+\kappa)^{4\nu+2}}e^{i\kappa\ell(2\nu+1)}. \qquad (2.26)$$

For our further calculations it is useful to write this as

$$\tilde{g}_{12}(\bar{x}^3, x^3) = \frac{2}{m_0^2}\sum_{\nu=0}^{\infty}\tilde{f}_\nu\left(\sqrt{\omega^2 - m_1^2}\right) \qquad (2.27)$$

with the new function $\tilde{f}_\nu$ given by

$$\tilde{f}_\nu(\omega) = (\omega^2 - m_0^2)e^{i\omega(\bar{x}^3-x^3-\ell)} \qquad (2.28)$$
$$\times \frac{-im_0^{4\nu+2}e^{i(2\nu+1)\ell\sqrt{\omega^2-m_0^2}}}{\sqrt{\omega^2-m_0^2}\left(\omega + \sqrt{\omega^2-m_0^2}\right)^{4\nu+2}}$$

and an effective cut-off frequency $m_0 = \sqrt{m_2^2 - m_1^2}$. Disregarding the factor ahead of the fraction in (2.28) for a moment, the function $\tilde{f}_\nu$ corresponds to the time domain function [13]

$$\mathcal{L}^{-1}\left[\tilde{f}_\nu(\omega)\frac{e^{-i\omega(\bar{x}^3-x^3-\ell)}}{\omega^2-m_0^2}\right] = \Theta\left(t - (2\nu+1)\ell\right)\left(\frac{t-(2\nu+1)\ell}{t+(2\nu+1)\ell}\right)^{2\nu+1}J_{4\nu+2}\left(m_0\sqrt{t^2 - (2\nu+1)^2\ell^2}\right), \qquad (2.29)$$

with the step function $\Theta(x)$ and the $\nu$th Bessel function $J_\nu(x)$.

The additional exponential factor only causes a time translation. By performing the inverse Laplace transformation $\mathcal{L}^{-1}$ one gets for $q_\nu(t, z) = \mathcal{L}^{-1}[\tilde{f}_\nu(\omega)(\omega^2 - m_0^2)^{-1}]$, with the abbreviation $z = \bar{x}^3 - x^3 > 0$, the solution

$$q_\nu(t, z) = \Theta(t - z - 2\nu\ell)\left(\frac{t-z+\ell-(2\nu+1)\ell}{t-z+\ell+(2\nu+1)\ell}\right)^{2\nu+1}J_{4\nu+2}\left(m_0\sqrt{(t-z+\ell)^2 - (2\nu+1)^2\ell^2}\right). \qquad (2.30)$$

Because of the remaining factor $\omega^2 - m_0^2$ the second time derivative of $q_\nu(t, z)$ enters the function $f_\nu(t, z) = \mathcal{L}^{-1}[\tilde{f}_\nu(\omega)]$. Due to the vanishing of the function $q_\nu(0, z)$ for the values $z + 2\nu\ell > 0$ no boundary terms arise from the Laplace transform of the second time derivative $\ddot{q}_\nu(t, z)$. Thus we have

$$f_\nu(t, z) = -m_0^2 q_\nu(t, z) - \ddot{q}_\nu(t, z). \qquad (2.31)$$

Now the inverse transform of the series in (2.27) yields for its terms, defined by $h_\nu(t, z) = \mathcal{L}^{-1}[\tilde{f}_\nu(\sqrt{\omega^2 - m_1^2})]$, the expression [13]

4

$$h_\nu(t,z) = f_\nu(t,z) - m_1 \int_0^t f_\nu\left(\sqrt{t^2-u^2},z\right) J_1(m_1 u)du. \tag{2.32}$$

Therefore we obtain for the integral (2.23) the series expansion

$$\begin{aligned}
g_{12}(t,z) &= \frac{2}{m_0^2} \sum_{\nu=0}^\infty h_\nu(t,z) \\
&= -2 \sum_{\nu=0}^\infty \left[ q_\nu(t,z) + \frac{1}{m_0^2} \ddot{q}_\nu(t,z) \right. \\
&\quad \left. -m_1 \int_0^t \left\{ q_\nu\left(\sqrt{t^2-u^2},z\right) + \frac{1}{m_0^2}\ddot{q}_\nu\left(\sqrt{t^2-u^2},z\right) \right\} J_1(m_1 u)du \right].
\end{aligned} \tag{2.33}$$

The structure of this Green's function can be explained phenomenologically by looking at Eq. (2.32). Even the leading term $q_0$ of the series, and thus $h_0$, jumps from zero to a finite value at the boundary of the past light cone. This property of Green's function guarantees the causal propagation of every pulse. In opposition to the free space here the support of Green's function is not only the boundary of the light cone but its full interior. There are two reasons for this feature. First, consider the first term in Eq. (2.32) and accordingly the terms of the series $q_\nu$ given by Eq. (2.30). These terms contribute to the series only when $t > z + 2\nu\ell$. Thus the $\nu$th term of the series represents the part of the field that leaves the barrier on the right hand side after $2\nu$ reflections at its boundaries. For the second reason take a look at the second term of Eq. (2.32). This term has nothing to do with the barrier itself but arises from the boundary conditions of the wave guide. Notice that the field is reflected there and back from the metallic boundaries while propagating through the waveguide. This echo effect is described by the integral of the term in question. This integral represents a distortion in which all excitations that are noticeable at a given position in the time interval $[0,t]$ take part.

## III. TUNNELING OF WAVE PACKETS

### A. Analysis

Now we will solve the Maxwell equations for a given pulse using Green's function determined in the last section. Before starting with this calculation we want to simplify Green's function. It has been noticed above that a distortion integral like that of Eq. (2.32) always arises in the case of guided waves. However, the tunneling effect itself is described completely by the functions $f_\nu(t,z)$ in the first term of Eq. (2.32). We are interested in the undistorted delay induced by the tunneling effect only. Therefore, in the following calculations we consider only this term of Green's function, i.e. we set

$$g_{12}(t,z) = -2 \sum_{\nu=0}^\infty \left\{ q_\nu(t,z) + \frac{1}{m_0^2}\ddot{q}_\nu(t,z) \right\} \tag{3.1}$$

to determine the influence of the barrier itself on the transmitted pulse. With this simplification, the studied system has been mapped onto the model investigated by Deutch and Low [11]. Their cut off frequency corresponds to our effective cut-off frequency $m_0 = \sqrt{m_2^2 - m_1^2}$. Notice that, for comparing with experimental results, the contribution of the distortion term to the total transmitted pulse decreases with an increasing difference between the lower cut-off frequency $m_1$ and the central frequency $\omega_0$ of the pulse.

Using now Eq. (2.3), (2.6) with the simplified form (3.1) of Green's function with $x^0 = 0$, we obtain the component $B_3$ behind the barrier for an arbitrary pulse started in front of the tunneling region. Our calculations will be carried out with a pulse given by a truncated Gaussian $H_{10}$-mode centered at some position $x^3 = s < -\ell/2$ in front of the barrier and with central frequency $\omega_0$ corresponding to the wavenumber $k_0 = \sqrt{\omega_0^2 - m_1^2}$. In this case the relevant and non vanishing field components [10] are the real parts of

$$E_2(x) = i\omega_0 \frac{a}{\pi} \sin(x^1\pi/a)\,\varphi(x^3) \tag{3.2}$$

$$B_3(x) = \cos(x^1\pi/a)\,\varphi(x^3) \tag{3.3}$$

with the Gaussian envelope

$$\varphi(x^3) = \Theta(-x^3 + s + \gamma)\,e^{ik_0 x^3} e^{-(x^3-s)^2/\sigma^2}. \tag{3.4}$$

The distance between the maximum and the wavefront of the packet is given by the parameter $\gamma$ with the property $0 < \gamma < -s - \ell/2$. The upper boundary of $\gamma$ comes from the condition that the wavefront of the initial pulse has to be in front of the barrier at $x^0 = 0$. This is necessary because the barrier causes deformations of the pulse which are initially unknown.

With this initial pulse one can carry out the integration in Eq. (2.3) using the convolution theorem. Changing the

integration variable to $v = t - \bar{x}^3 + \ell$, we find the final solution for the component $B_3$ of the pulse behind the barrier. With the relative coordinate $u = \bar{x}^0 - \bar{x}^3 + s + \ell$ one gets

$$B_3(\bar{x}) = -\cos(\bar{x}^1\pi/a)\frac{2}{m_0^2}\sum_{\nu=0}^{\infty}\left[\cos(k_0(u-s))\Gamma_\nu^{(1)}(u) + \sin(k_0(u-s))\Gamma_\nu^{(2)}(u)\right] \tag{3.5}$$

with

$$\Gamma_\nu^{(1,2)}(u) = \Theta(u + \gamma - (2\nu+1)\ell)\int_{(2\nu+1)\ell}^{u+\gamma} e^{-(u-v)^2/\sigma^2}\left(\frac{v - (2\nu+1)\ell}{v + (2\nu+1)\ell}\right)^{2\nu+1}$$

$$\times J_{4\nu+2}\left(m_0\sqrt{v^2 - (2\nu+1)^2\ell^2}\right)\left(\cos(k_0v)\vartheta^{(1,2)}(u-v) \mp \sin(k_0v)\vartheta^{(2,1)}(u-v)\right)dv, \tag{3.6}$$

and the abbreviations

$$\vartheta^{(1)}(t) = \frac{2}{\sigma^2}t\left(\omega_0^2 - m_2^2 + 2k_0(k_0 + \omega_0) - \frac{4t^2}{\sigma^4} + \frac{6}{\sigma^2}\right) \tag{3.7}$$

$$\vartheta^{(2)}(t) = k_0\left(\omega_0^2 - m_2^2 - \frac{12t^2}{\sigma^4} + \frac{6}{\sigma^2}\right) + \omega_0\left(\omega_0^2 - m_2^2 - \frac{4t^2}{\sigma^4} + \frac{2}{\sigma^2}\right). \tag{3.8}$$

The integral in Eq. (3.6) can be evaluated only numerically. Note that, for a fixed value of $u$, all of the functions $\Gamma_\nu^{(1,2)}(u)$ with an index $\nu$ larger than some index $\nu_0$ vanish. Naturally, the index $\nu_0$ depends on the value of $u$. So we have to do only a finite number of numerical integrations to obtain the component $B_3$. The envelope of $B_3$ is shown in Fig. 2 for different barrier thicknesses $\ell$ and fixed central and cut-off frequencies. The distance $\gamma$ between the maximum and the wave front of the wave packet has to be large enough to prevent deformations of the transmitted pulse that arise in the case of a pulse with too large high-frequency components. For this and the following results $\gamma$ has been chosen to be five times the initial variance $\sigma_0$ of the pulse. Due to the trivial dependence of the solution on the coordinate $x^1$ we have always set $x^1 = 0$ corresponding to the boundary of the waveguide. Because we have eliminated the echo effect caused by the waveguide itself, the pulse does not change its shape outside the barrier region. Thus the graphs in Fig. 2 correspond to the time evolution of the wave packet measured by an observer at an arbitrary position behind the barrier. To determine the tunneling time of the maximum of the wave packet, we can use the free propagation of the wave packet outside the barrier, i.e. the fact that it travels there with the vacuum speed of light without changing its shape. Then the maximum of the packet arrives at the left end of the barrier at $x^0 = -s - \ell/2$. Now let $\tau$ be the value of $u$ at which the envelope of $B_3(u)$ has its maximum. Considering the definition of the coordinate $u$, one obtains for the arrival time at the right end of the barrier $x^0 = \tau - s - \ell/2$. Thus the tunneling time is given by $\tau$.
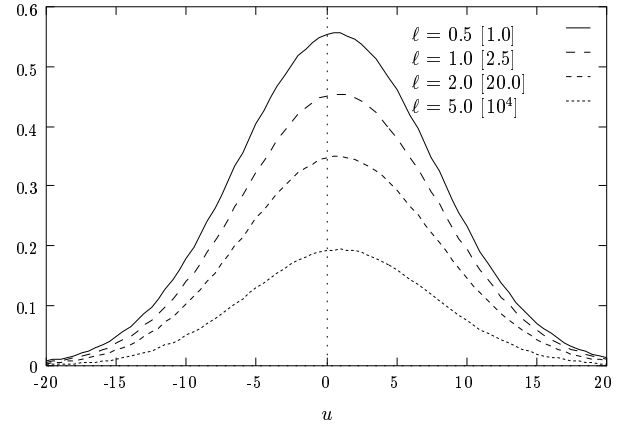


FIG. 2. Graphs of the envelope of the component $B_3$ of the magnetic field for Gaussian wave packets transmitted below cut-off across barriers of different thickness $\ell$ as a function of the relative coordinate $u$. The cut-off frequencies are $m_1 = 1$ and $m_2 = 4$. In all cases $\omega_0 = 3.2$ and $\sigma = 10$. The graphs are scaled by the factors in the brackets.

The graphs in Fig. 2 show that the transmitted pulses are also Gaussian-like wave packets, but exponentially damped with growing barrier thickness. To obtain the tunneling time and the variance of the packets we have fitted Gaussian wave packets to the graphs of Fig. 2. The resulting values for $\tau$ and the variance $\sigma$ are listed in Table I. Furthermore, this table shows values also corresponding to Gaussian-like solutions for other cut-off fre-

6

quencies of which the graphs are not shown here. While in the case of $\ell = 0.5$ the tunneling time corresponds to a subluminal average velocity of the maximum, it increases more and more slowly with growing barrier thickness. This result agrees with the experimental observation that for sufficiently long barriers the tunneling time is independent of thickness [5]. The variance of the transmitted wave packets decreases with increasing barrier thickness.

To determine the dependence of the tunneling time on the central frequency of the initial pulses we have calculated the corresponding transmitted wave packets for a barrier of fixed thickness $\ell = 5$ with $m_1 = 1$ and $m_2 = 4$. We have considered Gaussians with variances both above ($\sigma_0 = 10$) and below ($\sigma_0 = 4$) the thickness. The resulting pulses are also Gaussian-like except for the low-variance-pulses with $\omega_0 \stackrel{>}{\sim} m_2/2$. The parameters of the Gaussian solutions are given by Table II. The tunneling time increases with the central frequency but corresponds always to a superluminal average velocity for the maximum of the pulse. The maxima are shifted to higher values of $\tau$ with increasing $\omega_0$ because of contributions from Fourier components above the barrier cut-off. These components are also responsible for the slightly higher times of the narrow packets and its distortion at higher central frequencies. The variance of the transmitted packets decreases with increasing $\omega_0$.

TABLE I. Numerical results for tunneling times and variances of wave packets that have crossed barriers of different length. Two different pairs of cut-offs are considered with a corresponding central frequency in between. In both cases the initial variance is $\sigma_0 = 10$.

| $\ell$ | $m_1 = 1, m_2 = 4$ | | $m_1 = 6.5, m_2 = 9.5$ | |
| | $\omega_0 = 3.2$ | | $\omega_0 = 8.5$ | |
| | $\tau$ | $\sigma$ | $\tau$ | $\sigma$ |
| 0.5 | 0.66 | 10.01 | | |
| 1.0 | 0.82 | 9.97 | | |
| 2.0 | 0.86 | 9.85 | | |
| 3.0 | | | 0.48 | 9.82 |
| 5.0 | 0.91 | 9.38 | 0.49 | 9.66 |

Let us now compare the tunneling times obtained from our solutions with that of Martin and Landauer [3]. These authors have pointed out that the time delay of the center of mass for a pulse restricted to a wide variance in the time domain depends only on the frequency derivative of the phase $\alpha$ of the transmission coefficient, i.e.

$$\tau_{\mathrm{ML}} = \frac{d\alpha}{d\omega} + \ell\frac{dk}{d\omega}, \qquad (3.9)$$

where the expression has to be evaluated at $\omega = \omega_0$. Due to the symmetry of the transmitted pulse the time delay for the center of mass and the maximum are the same. But the time $\tau_{\mathrm{ML}}$ does not represent the pure time delay of the maximum caused by the barrier itself: Due to the echo effect of the waveguide which also affects the transmission coefficient, $\tau_{\mathrm{ML}}$ is shifted to higher values. To account for this fact, we compare the tunneling times of our echo-free solutions with that of Martin and Landauer by taking in Eq. (3.9) the phase of the transmission coefficient with $m_1 = 0$, corresponding to a free propagation outside the barrier. The graph of $\tau_{\mathrm{ML}}$ and our values of $\tau$ are plotted in Figs. 3 and 4 as functions of the central frequency and the barrier thickness, respectively, for the parameters considered above. A difference between the two tunneling times arises only for higher central frequencies because of the growing contribution of high Fourier components to the transmitted pulse. Notice that the approximate result of Martin and Landauer is valid only for pulses with a narrow frequency range. Furthermore our values for the tunneling time retains a small dependence on thickness, but corresponds nevertheless to a superluminal velocity for the maximum of the pulse. At this moment it should be emphasized again that the wave front travels always with the vacuum speed of light. Below, the possibility of superluminal maxima within an underlying causal propagation will be explained in terms of the energy flow across the barrier.

TABLE II. Numerical results for tunneling times and variances of wave packets with different central frequencies between both cut-offs and initial variance $\sigma_0 = 10$ and $\sigma_0 = 4$, respectively. The barrier thickness is $\ell = 5$.

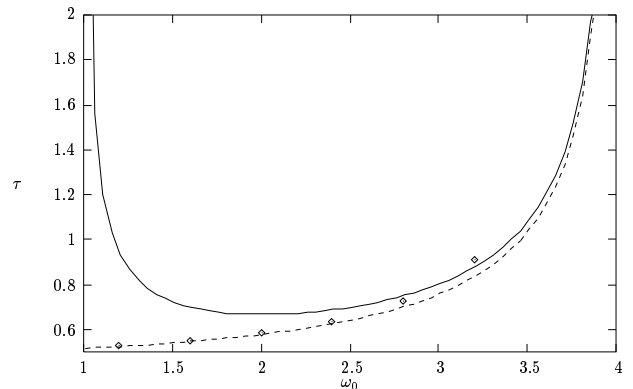| $\omega_0$ | $\sigma_0 = 10$ | | $\sigma_0 = 4$ | |
| | $\tau$ | $\sigma$ | $\tau$ | $\sigma$ |
| 1.2 | 0.52 | 9.90 | 0.53 | 3.72 |
| 1.6 | 0.55 | 9.87 | 0.57 | 3.61 |
| 2.0 | 0.58 | 9.83 | 0.63 | 3.43 |
| 2.4 | 0.64 | 9.78 | | |
| 2.8 | 0.72 | 9.68 | | |
| 3.2 | 0.91 | 9.38 | | |



FIG. 3. Graph of the tunneling time for a wave packet calculated by Martin and Landauer [3] from the frequency derivative of the phase of the transmission coefficient as a function of the central frequency of the packet. Solid line: The cut-off frequencies are $m_1 = 1$, $m_2 = 4$ and the barrier thickness is $\ell = 5$. The dashed line corresponds to a vanishing cut-off frequency outside the barrier ($m_1 = 0$). The dots represent the tunneling time of the maximum of our solution given by Eq. (3.5) with $\sigma_0 = 10$.
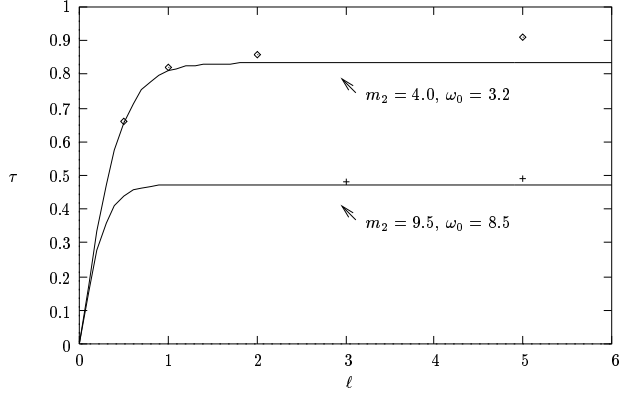
7

FIG. 4. Graphs of the tunneling time as given both by [3] with vanishing cut-off frequency $m_1$ outside the barrier (lines) and by the maximum of the solution (3.5) (dots) as a function of the barrier thickness for two different pairs of cut-off frequencies and a central frequency in between. The dots correspond to the values given in Table I.

### B. Interpretation

Apparently, the maxima of the solutions we have given above cross the barrier with a superluminal velocity. In this section, we want to explain this property of the transmitted wave packet in terms of the energy flow across the barrier. In Minkowskian space-time it is given by the integral curves of the 4-vector field $\mathcal{T}^\alpha$ with the electromagnetic energy density $\mathcal{T}^0 = \frac{1}{2}(\vec{E} \cdot \vec{D} + \vec{B} \cdot \vec{H})$ and the Poynting vector $\mathcal{T}^j = (\vec{E} \times \vec{H})_j$ for $j = 1, 2, 3$.

The fact that $\mathcal{T}^\alpha$ is a continuous differentiable vector field induces an important property of its integral curves in space-time: Curves with different initial positions do not intersect each other. This property is not destroyed by the jumping conditions for the electromagnetic field at the ends of the barrier. To prove this claim we have to show only that any curve flowing on a boundary of the barrier from one side has a unique continuation at the other side of the boundary. This means that there are no branching points for the curves at the boundary. Due to the continuity of the component $\mathcal{T}^3$ at the boundary these points could only arise if one assumed that the component $\mathcal{T}^3$ vanished there and thus on both sides the curves were tangential to the boundary at this position of space-time. This would be the case for a curve that comes, for example, from the right, is tangent to the boundary and than goes back to the right. At the position where the curve is tangential to the boundary, another curve could flow into this curve from the other side of the boundary, leading to a branching point. But this situation is not possible because the tangential vectors of the curves have to point in the directions of the future light cone. Looking at the neighboring curves of those considered above, these possible directions would

be inconsistent with the continuity of $\mathcal{T}^3$ and the fact that the curves do not intersect each other outside the boundary. Thus there are no branching points at the boundary.
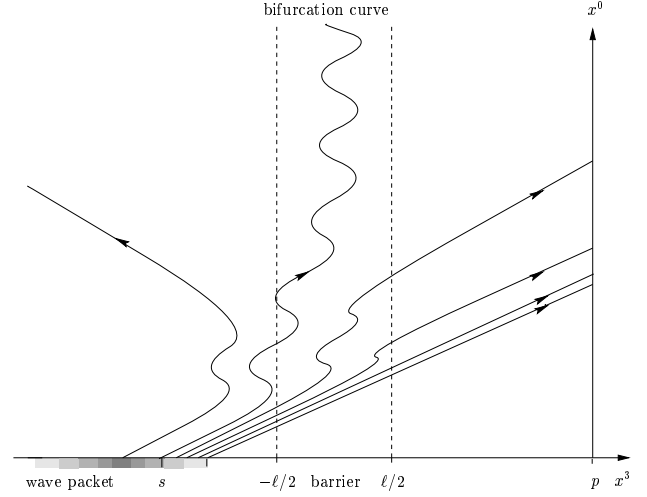


FIG. 5. A qualitative plot of the energy flow in a $x^0$-$x^3$-plane of the Minkowskian space-time. The plot intensity of the initial wave packet corresponds to its energy density.

So we obtain the qualitative picture for the integral curves of the energy flow in the space-time shown in Fig. 5. The curves originate in the initial pulse of which the wave front is still to the left of the barrier at time $x^0 = 0$. The curve originating in the wave front of the pulse has a slope of one because the wave front propagates with the vacuum speed of light. The fact that the curves do not intersect each other allows the initial pulse to be decomposed into two connected parts from which transmitted and reflected curves, respectively, originate. If there is no energy absorbed by the barrier, the starting position $s$ of the bifurcation curve separating transmitted and reflected curves is given implicitly by the transmitted portion of the energy of the initial pulse, i.e.

$$\int_s^\infty \mathcal{T}^0_{|x^0=0} dx^3 = \int_0^\infty \mathcal{T}^0_{|x^3=p} dx^0. \qquad (3.10)$$

The integration along the time axis can be done at any position $x^3 = p$ behind the barrier.

Now, by means of the energy flow as shown in Fig. 5, we want to explain the existence of solutions with superluminal maxima within a causal theory. The part of the initial pulse between its wave front and the starting point $s$ of the bifurcation curve is mapped along the energy flow on the time axis at $x^3 = p$. The closer two neighboring points of the initial pulse at $x^0 = 0$ are to the starting point $s$ of the bifurcation curve, the more the distance between them is extended by this mapping.

This is necessary because of the arrival of transmitted curves at $x^3 = p$ also at arbitrary late times. Due to this spreading of the curves the energy density of the transmitted pulse at $x^3 = p$ begins to decrease from a particular time corresponding to the arrival time of the maximum behind the barrier. In other words, the transmitted pulse results from a redistribution of the energy contained in the forward tail between the front and $s$ of the starting pulse. Thus the maxima of the initial and transmitted pulse are not causally related.

The whole picture arises as a consequence of the mathematical claim that the curves do not intersect each other. These curves themselves, of course, cannot be observed in any experiment. But we believe that they are a suitable tool to get a classical picture of the mechanism of the tunneling effect. Within this classical interpretation the surprising result of our solutions is the almost exact reconstruction of a Gaussian wave packet behind the barrier. This effect yields a pulse-reshaping [1].

To obtain a more physical point of view one can ask at which time the transmitted pulse exceeds an arbitrary threshold behind the barrier. Due to the damping and squeezing of the transmitted pulse this happens always at a later time compared to a pulse which crosses no barrier. That means for an observer behind the barrier that he would not detect the tunneled pulse earlier than the freely propagated one, in agreement with causality.

## IV. SUMMARY AND CONCLUSION

In Eq. (3.5), we have given an exact analytic expression in the time domain for the causal Green's function of a model that describes an ideal case of electromagnetic tunneling. The structure of this function allows for a reduction to those terms which describe only the pure tunneling effect without the distortions caused by the waveguide. With this reduced Green's function, we calculated the shape of transmitted wave packets for truncated Gaussians as initial pulses. The resulting pulse can be also Gaussian-like. In agreement with the approximate result of Martin and Landauer [3] and the experiments on microwaves by Enders and Nimtz [5], the time delay of the maximum of the pulse becomes nearly independent of the thickness for sufficiently long barriers. Furthermore, the variance of the transmitted packet decreases with increasing barrier thickness. By examining the properties of the energy flow, we have found consistency of a superluminal pulse maximum with the causality of Maxwell's theory.

Within this interpretation the energy of the transmitted pulse can only originate from a connected part behind the wave front of the initial wave packet because the integral curves of the energy flow do not intersect each other. In this sense, the Gaussian shape of the transmitted pulse can only be interpreted as an amazing interference effect. Due to the propagation of the wave front with the vacuum speed of light, it is not possible to obtain a superluminal maximum if the barrier thickness exceeds the distance between the maximum and the wave front. Thus, in the case of truncated wave packets, the time delay of the maximum does not stay independent of the thickness for all barrier length. In summary, the results of the tunneling experiments can be obtained from the causal Maxwell theory.

[1] T.E. Hartman, J. Appl. Phys. **33** (1962) 3427.
[2] S. Bosanac, Phys. Rev. A **28** (1983) 577.
[3] Th. Martin, R. Landauer, Phys. Rev. A **45** (1992) 2611.
[4] A. Enders and G. Nimtz, J. Phys. I (France) **2** (1992) 1693.
[5] A. Enders and G. Nimtz, Phys. Rev. E **48** (1993) 632.
[6] A. Enders and G. Nimtz, Phys. Rev. B **47** (1993) 9605.
[7] A. Enders and G. Nimtz, J. Phys. I (France) **3** (1993) 1089.
[8] G. Nimtz, A. Enders and H. Spieker, J. Phys. I (France) **4** (1994) 565.
[9] H.M. Brodowsky, W. Heitmann and G. Nimtz, submitted to Phys. Lett. A.
[10] D. Jackson, *Classical Electrodynamics* (Wiley, New York 1975).
[11] J.M. Deutch and F.E. Low, Ann. Phys. (New York)**228** (1993) 184.
[12] W. Thirring, *A Course in Mathematical Physics, Vol. 2* (Springer, New York 1979).
[13] H. Bateman, *Tables of Integral Transforms I* (McGraw-Hill Book Company, New York 1954).